



Direct evidence of fadeout of collective enhancement in nuclear level density



K. Banerjee ^{a,b,*}, Pratap Roy ^{a,b}, Deepak Pandit ^a, Jhilam Sadhukhan ^{a,b}, S. Bhattacharya ^a, C. Bhattacharya ^{a,b}, G. Mukherjee ^{a,b}, T.K. Ghosh ^{a,b}, S. Kundu ^{a,b}, A. Sen ^{a,b}, T.K. Rana ^a, S. Manna ^{a,b}, R. Pandey ^a, T. Roy ^{a,b}, A. Dhal ^a, Md.A. Asgar ^{a,b}, S. Mukhopadhyay ^{a,b}

^a Variable Energy Cyclotron Centre, 1/AF-Bidhannagar, Kolkata 700064, India

^b Homi Bhabha National Institute, Training School Complex, Anushaktinagar, Mumbai 400094, India

ARTICLE INFO

Article history:

Received 11 May 2017

Received in revised form 31 May 2017

Accepted 12 June 2017

Available online 15 June 2017

Editor: V. Metag

Keywords:

Nuclear level density

Statistical compound-nucleus reactions

Neutron spectroscopy

Liquid scintillator based neutron detectors

ABSTRACT

The phenomenon of collective enhancement in nuclear level density and its fadeout has been probed using neutron evaporation study of two strongly deformed (^{173}Lu , ^{185}Re), and one spherical (^{201}Tl) compound nuclei over the excitation energy (E^*) range of $\sim 22\text{--}56$ MeV. Clear signature of the fadeout of collective enhancement in nuclear level density was observed for the first time in both the deformed evaporation residues ^{172}Lu and ^{184}Re at an excitation energy range $\sim 14\text{--}21$ MeV. Calculations based on finite temperature density functional theory, as well as macroscopic–microscopic shape transition model, have strongly established a close correlation between the observed fadeout of collective enhancement and a deformed to spherical nuclear shape transition in these nuclei occurring in the same excitation energy zone. Interestingly, a weak signature of fadeout has also been observed for the spherical residue ^{200}Tl . This is due to a similar shape transition of the deformed excited state configuration of ^{200}Tl .

© 2017 The Authors. Published by Elsevier B.V. This is an open access article under the CC BY license (<http://creativecommons.org/licenses/by/4.0/>). Funded by SCOAP³.

Understanding the single particle and collective properties of atomic nuclei in general, and nuclear level density (NLD) in particular is of utmost importance for proper quantitative explanation of a wide range of physical processes in nuclear physics, astrophysics as well as nuclear technology. The manifestation of the two (single particle and collective) properties may sometimes be closely interlinked; this is at least the case for nuclear level density, where the degree of mixing is decided by the intricate interplay of single-particle and collective excitations [1–3]. Consequently, it was predicted, both phenomenologically as well as microscopically [4–7], that there should be an enhancement of NLD over its single particle value due to collectivity, which would subsequently get damped at higher excitation. This phenomenon of enhancement and its fadeout in NLD is assumed to depend on various factors like ground state deformation, excitation energy of the nucleus under consideration. The fadeout of collective enhancement in NLD is however, yet to be 'observed' experimentally. An unambiguous experimental confirmation of its existence is crucial for the validation of theoretical models as well as for realistic prediction of impor-

tant reaction rates, cross sections, which are required in various areas of current interest, from the synthesis of superheavy nuclei to stellar nucleosynthesis problems. In the present letter, we report such a direct experimental evidence of collective enhancement in NLD and its fadeout in highly deformed nuclei. Microscopic origin of this phenomenon is also explained with theoretical calculations.

Phenomenologically, collective contribution in the nuclear level density $\rho(E^*, J)$ at excitation energy E^* and angular momentum J is expressed as [4],

$$\rho(E^*, J) = \rho_{\text{int}}(E^*, J)K_{\text{coll}}(E^*), \quad (1)$$

where $\rho_{\text{int}}(E^*, J)$ is the intrinsic single particle level density, and $K_{\text{coll}} (= K_{\text{rot}}K_{\text{vib}})$, K_{rot} , K_{vib} are the total, rotational and vibrational enhancement factors, respectively. Microscopic shell model studies [5] have predicted that, for nuclei with finite ground state deformation, rotational collectivity causes large enhancement of NLD ($K_{\text{rot}} \sim 100$) up to moderate excitation (typically, $\sim 20\text{--}30$ MeV). In comparison, $K_{\text{vib}} \ll K_{\text{rot}}$ is negligible ($\simeq 1$) except at very low excitations (typically $\lesssim 5$ MeV). Beyond a critical value of excitation energy (temperature), E_{cr}^* (T_{cr}), the enhancement fades out ($K_{\text{coll}}(E_{\text{cr}}^*) \simeq 1$) and NLD is purely of single particle in nature. This phenomenon is predicted to be due to the deformed to spheri-

* Corresponding author at: Variable Energy Cyclotron Centre, 1/AF-Bidhannagar, Kolkata 700064, India.

E-mail address: kaushik@vecc.gov.in (K. Banerjee).

cal shape phase transition of the nucleus when it can no longer support rotational bands [6,8,9,7]. Microscopic calculations indicated that this fadeout transition is fairly sharp and takes place at a critical energy $E_{cr}^* \sim 18\text{--}25$ MeV [6,9]. Phenomenologically it was estimated that this transition may be represented by a Fermi distribution-like function with a critical energy $E_{cr}^* \sim 120A^{1/3}\beta^2$ [5]. In an another independent work Björnholm et al. have estimated the critical temperature $T_{cr} \sim 40A^{-1/3}\beta$ MeV for this transition, where β is the ground-state deformation [10]. However, the sharpness of this transition may be considerably blurred if thermal shape fluctuations are incorporated in the calculation, as will be shown later.

On the experimental front, however, the phenomenon of damping of collectivity and vis-a-vis the fadeout of collective enhancement in NLD has so far eluded direct detection. An indirect signature of collective enhancement was obtained by Junghans et al. to explain the production cross sections of projectile-like fragments produced in high energy fragmentation of uranium and lead [11]. On the other hand, the attempt to extract direct evidence of enhancement and its fadeout from α -particle evaporation study of the compound nucleus $^{178}\text{Hf}^*$ ($\beta = 0.278$) yielded a null result [12]. However, our recent neutron evaporation study on axially deformed nuclei, $^{185}\text{Re}^*$ and $^{169}\text{Tm}^*$, has provided positive indications of the onset of the phenomenon, though proper identification of the transition zone could not be possible due to limited range of the data [13]. Therefore, the challenge is two-fold: firstly, to extract direct experimental evidence on the fadeout of enhancement of NLD at higher excitation by identifying the transition zone, and secondly to establish its link with the damping of collectivity and, vis-a-vis, a deformed to spherical shape transition of the nucleus. In this letter, we present the first direct evidence on the existence of fadeout of collective enhancement in NLD in deformed ^{172}Lu and ^{184}Re nuclei from an experimental study of respective evaporation neutron energy spectra from the corresponding compound nuclei. The correlation between the observed fadeout of collectivity and shape transition in these nuclei has also been investigated in the framework of two theoretical approaches: the Finite Temperature Density Functional Theory (FT-DFT) [14–17] and the macroscopic–microscopic shape phase transition model (MMSTM) [18–20]. Surprisingly, even in the case of spherical ^{200}Tl , a weak but distinct signature of enhancement and the fadeout was visible; this has been explained in terms of nuclear structure consideration [21,22].

The prime objective of the present experiment was to probe the variation of level density parameter a directly from the respective backward angle neutron evaporation data for both deformed and non-deformed nuclei over the whole range of excitation energy of interest (encompassing the transition zone: $E^* \sim 20\text{--}50$ MeV). The experiment was carried out using ^4He ion beams of incident energies in the range of 26–60 MeV from the K130 cyclotron at the Variable Energy Cyclotron Centre (VECC), Kolkata. Self-supporting foils of ^{169}Tm (thickness ~ 1.15 mg/cm 2), ^{181}Ta (thickness ~ 1.3 mg/cm 2) and ^{197}Au (thickness ~ 3.1 mg/cm 2) were used as targets to populate the compound nuclei $^{173}\text{Lu}^*$ ($\beta \sim 0.286$), $^{185}\text{Re}^*$ ($\beta \sim 0.221$) and $^{201}\text{Tl}^*$ ($\beta \sim -0.044$), respectively in the excitation energy range $\sim 22\text{--}56$ MeV [23]. The emitted neutrons were detected using four liquid scintillator detectors [24] placed at the laboratory angles of 90° , 105° , 120° and 150° at a distance of 1.5 m from the target except for the measurement at lowest beam energy of 26 MeV, where the detectors were kept at 75 cm from the target. Energies of the emitted neutrons were measured by the time-of-flight (TOF) technique, where each valid start of the TOF was generated from a 50-element BaF₂ γ -ray detector array when at least two detectors of the array fired simultaneously [25]. The BaF₂ array was split into two equal parts which were

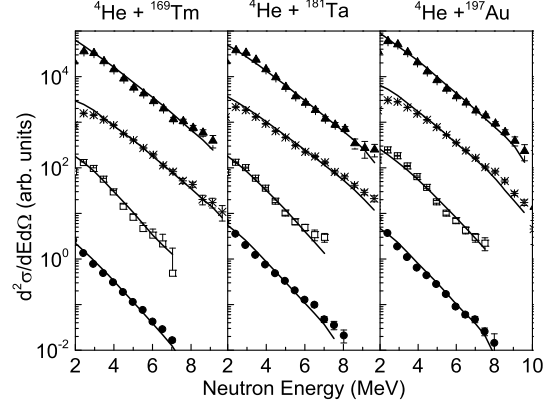


Fig. 1. Measured neutron energy spectra (symbols) at four incident energies shown along with the respective statistical model fits (curves). Solid circle, hollow square, star and solid triangle represent data at incident energies of 26, 30, 35 and 40 MeV respectively.

placed in staggered-castle type geometry, on top and bottom sides of the thin walled target chamber. The neutron and γ separation was achieved by both TOF and pulse shape measurements. Details of the experimental technique have already been described in our earlier papers [13,26–28].

The neutron data at the most-backward angle (150°) were used for the present analysis as the contribution of any direct component is minimum at this angle. To focus on the possible transition zone, the extracted centre of mass (c.m.) neutron kinetic-energy spectra from the decay of $^{173}\text{Lu}^*$, $^{185}\text{Re}^*$ and $^{201}\text{Tl}^*$ at four lowermost incident energies of 26, 30, 35 and 40 MeV have been displayed in Fig. 1. The slopes of the spectra at 26 and 30 MeV are distinctly different from those at 35 and 40 MeV for all the three cases. The experimental neutron energy spectra were compared with the respective statistical model (SM) calculations using the code GEMINI++ [29]. Here, $\rho_{int}(E^*, J)$ is calculated using back shifted Fermi gas model [30]. Shell effect and its washing out with excitation energy was incorporated using the energy dependent level density parameter $a = \tilde{a} f(U, J, \delta W, \gamma)$, $U = E^* - E_{rot}(J) + \delta P$, $E_{rot}(J)$ being the rotational energy and δP the pairing correction. Function $f(U, J, \delta W, \gamma)$ incorporates the effects of shell correction and its damping at higher excitation, where δW and γ are the shell correction energy and shell damping coefficient, respectively [29,31]. The shape of the neutron evaporation spectrum is mostly determined by the value of the level density parameter which was estimated in terms of the best-fit values of $\tilde{a} = A/k$, where k is called the inverse level density parameter and \tilde{a} is the asymptotic (intrinsic) value of a at high excitation energies. The best-fit values of k for all the three systems at various excitation energies are shown in Fig. 2.

In the compound nuclear decay process, neutrons are emitted from different stages of the decay cascade. Therefore, the average thermal excitation energy $\langle U \rangle$ was estimated using $\langle U \rangle = \sum(U_i w_i)/\sum(w_i)$, where U_i is the excitation energy of the i -th nuclei in the decay chain and w_i is the corresponding yield of neutrons. The average residue $\langle A \rangle$ was calculated in the same the way, which were ^{172}Lu , ^{184}Re and ^{200}Tl up to 35 MeV beam energy, and ^{171}Lu , ^{183}Re and ^{199}Tl above 35 MeV (except 60 MeV). However, it is interesting to note that all the isotopes of Lu, Re, and Tl in the decay chain are having similar ground state deformation [23].

It is evident from the Fig. 2 that, for the decay of deformed nuclei $^{173}\text{Lu}^*$ and $^{185}\text{Re}^*$, there is a sharp change (relative increase) in the value of inverse level density parameter k within the compound nuclear excitation energy interval of 27–37 MeV, which

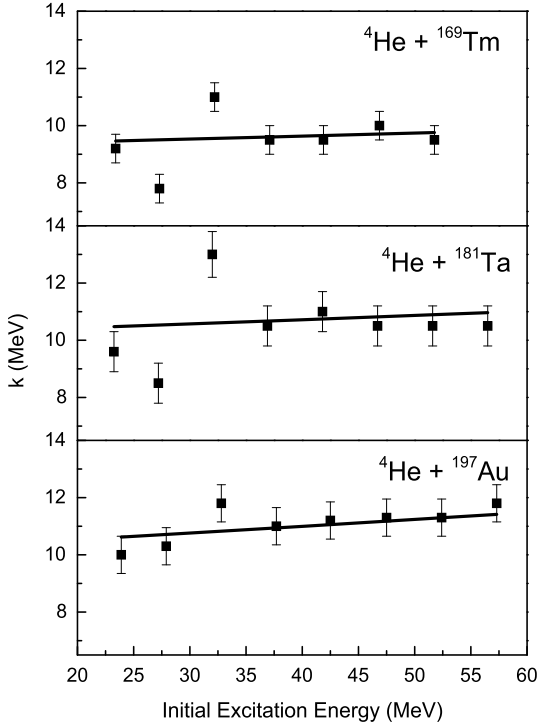


Fig. 2. Inverse level density parameter plotted as a function of initial excitation energy of the compound nuclei. Experimental points are shown in symbols, lines represent systematics (see text).

corresponds to $\langle U \rangle \sim 14\text{--}21 MeV for evaporation residues (ER) ^{172}Lu and ^{184}Re . This amounts to an abrupt decrease in NLD in both the deformed cases at $\langle U \rangle \sim 14\text{--}21$ MeV. This sudden fall of NLD is a signature of fadeout of collective enhancement in NLD. Interestingly, in case of spherical nucleus $^{201}\text{Tl}^*$ too, a weaker but distinctly abrupt variation of k is observed in the same excitation energy region. Excluding this transition zone, the overall trend of k as a function of excitation energy matches with the standard empirical systematics $k_s(U) = k_0 + \kappa(U/A)$, as shown by the continuous line in the Fig. 2 [28,29]. This signifies that, beyond the fadeout region, NLD is purely single particle in nature. This is a clear and most direct signature of fadeout of collectivity in NLD in the two deformed nuclei – provided the observation of similar, though weaker, signature of fadeout for spherical nucleus ^{200}Tl can be explained properly. Interestingly, though all three systems were having different ground state deformations, the transition seems to occur at nearly same excitation energy region. This will be discussed further in the following paragraphs.$

In statistical model, the temperature is related to NLD by the relation,

$$\frac{1}{T} = \frac{d \ln \rho}{d \langle U \rangle}. \quad (2)$$

So any abrupt variation in NLD would reflect a similar variation in the temperature, which is likely to provide another direct signature of fadeout of collective enhancement. Assuming complete thermalisation, the apparent temperatures T_{app} have been extracted by fitting evaporated neutron energy spectra using Maxwell distribution, which are shown as function of $\langle U \rangle$ in the Fig. 3. Data were also fitted with $T_{app} \propto \sqrt{\langle U \rangle}$ distribution. It is clear from Fig. 3 that there is a significant deviation (rise) in T_{app} from the empirical systematics ($T_{app} \propto \sqrt{\langle U \rangle}$) for both ^{172}Lu and ^{184}Re nuclei in the excitation energy range 14–21 MeV, whereas a weaker (but identifiable) deviation is also observed for the nucleus $^{200}\text{Tl}^*$. The observed hump in T_{app} corresponds to a sudden change in NLD

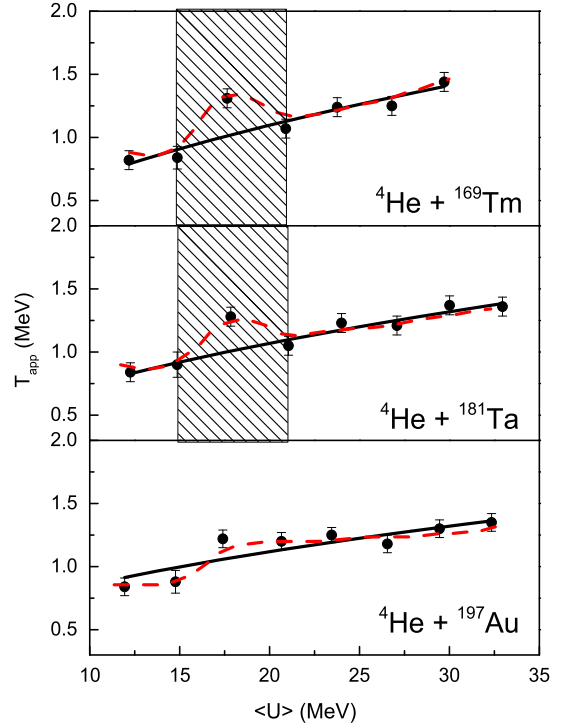


Fig. 3. (Colour online.) Apparent temperature as a function of average excitation energy of the daughter nuclei. Symbols are experimental points, solid lines represent systematics, and dotted lines are to guide the eye. Shaded region is the fadeout zone.

(from Eq. (2)), which provides another clear and straightforward signature of fadeout of collective enhancement in NLD for the deformed Lu and Re nuclei. At the same time, the conjecture of something similar also happening for ^{200}Tl , though on a weaker scale, is not ruled out.

It is very interesting to note here that the change over in inverse level density parameter k and temperature T is taking place in the excitation energy region where Giant Dipole Resonance (GDR) occurs [32], which is a collective phenomenon in atomic nuclei. GDR decay built on excited states competes with the neutron decay but with small branching ratio. Thus, in order to study the effect of GDR emission, the statistical model calculations were carried out by including the GDR decay using our recent measurements with alpha beams [33]. It was observed that the GDR branching ratio is very small $\Gamma_\gamma/\Gamma_n \sim 10^{-4}$ for both ^{173}Lu and ^{201}Tl at 26 and 50 MeV, which clearly indicates that GDR decay has negligible effect on the neutron evaporation spectra.

The microscopic origin of the fadeout of collective enhancement in NLD was investigated under the framework of finite temperature density functional theory [14–17] using the symmetry-unrestricted DFT solver HFODD (v 2.73y) [34]. The static (equilibrium) deformation β_{eq} of the system at each temperature was extracted by minimising V_0 , the difference between the (deformed) ground-state free energy and that corresponding to spherical shape. V_0 is the measure of dynamical hindrance for the excited nucleus to reach the spherical configuration. The transition point corresponds to the temperature when $T_{cr} \sim V_0$, where the effective hindrance vanishes and the system can move towards spherical shape due to thermal fluctuation. V_0 as a function of temperature is shown in Fig. 4 (inset). The evolution of β_{eq} as a function of temperature has been shown in Fig. 4 (upper). It is evident from the figure that such transition takes place as the temperature goes above 1.7 MeV for ^{172}Lu and ~ 1.3 MeV for ^{184}Re , which is very close to the temperature of our concern. In addition, an excited

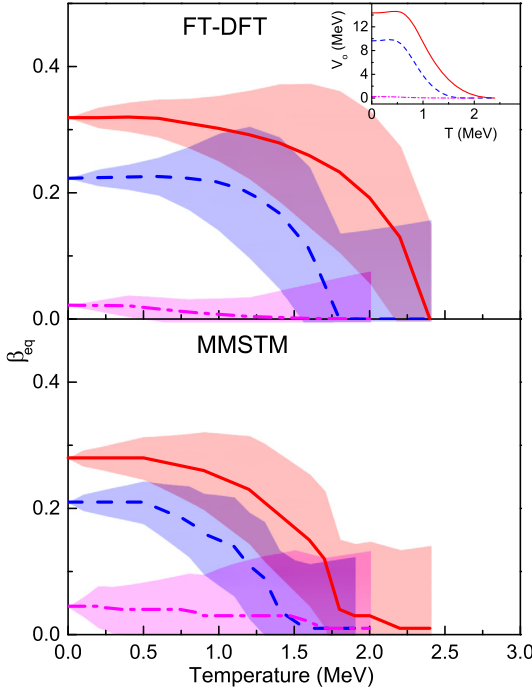


Fig. 4. (Colour online.) Equilibrium deformation β_{eq} (curve) and the corresponding thermal shape fluctuation (shaded area) plotted as a function of temperature. Solid (red), dash (blue) and dash dotted (pink) lines represent ^{172}Lu , ^{184}Re and ^{200}Tl , respectively. The variation of V_0 with temperature is shown in the inset.

system can also access different configurations leading to thermal shape fluctuations ($\Delta\beta$) around β_{eq} . The evolution of $\Delta\beta$ as a function of temperature has been illustrated in Fig. 4. It is seen that $\Delta\beta$ grows with temperature and beyond some point ($\gtrsim 0.8$ MeV), shape evolution profiles of the two systems significantly overlap, leading to washing out of the variation of T_{cr} between the two systems. This explains the present experimental observation of same fadeout transition zone in both systems. Independent theoretical calculation using macroscopic–microscopic shape phase transition model [18–20] also produced almost identical result (see Fig. 4 (lower)).

At this point, the case of spherical ^{200}Tl needs special attention. As expected, the above theoretical calculations do not predict any signature of shape transition in ^{200}Tl , though the data indicate the presence of weak shape transition in this case too. The ground state shape of all Tl nuclei are known to be spherical; however, ^{200}Tl becomes deformed at very low excitation energy of about 1 MeV due to the large deformation driving effect of the $h_{9/2}$ intruder orbital. The effect of the high-j intruder proton $h_{9/2}$ orbital and neutron $i_{13/2}$ orbital is inducing deformed shapes in both odd–even and odd-nuclei persists up to ^{201}Tl [22]. The deformed shapes are experimentally realised from the observation of rotational bands in ^{200}Tl having oblate deformation of $\beta \sim 0.1$ [21]. This explains the observation weak fadeout signature in ^{200}Tl though it is spherical in the ground state; it further establishes the correlation between the enhancement of NLD and deformation.

In summary, sudden increase in inverse level density parameter k and temperature T indicates the fadeout of collective enhancement in NLD for deformed nuclei ^{172}Lu and ^{184}Re . In the case of spherical nucleus ^{200}Tl too, a weaker signature of enhancement and fadeout of NLD was seen. The definite signature of fadeout (sudden drop of NLD) was observed in the average excitation energy range of 14–21 MeV, irrespective of the mass number or deformation of the nuclei. The experimental trends have been

qualitatively confirmed by two microscopic theories (FT-DFT and MMSTM), both of which predict deformed to spherical shape transition for ^{172}Lu and ^{184}Re at a temperature which is close to the observed fadeout temperature. The presence of thermal shape fluctuation leads to blurring of the sharpness of the transition, which explains the observation of the almost same fadeout zone irrespective of deformation. Moreover the admixture of higher chance neutron emission in the evaporation spectra leads to further blurring of transition zone information. In the case of spherical nucleus ^{200}Tl also, the apparently contradictory observation of weak signature of enhancement of NLD can be explained in terms of shape transition of the deformed excited state configuration of ^{200}Tl originating from its shell structure. Therefore, it may be concluded that the observation of fadeout transition in all the three cases and their correlation with the deformed to spherical shape transition are unequivocally established through the present experimental study for the first time.

The authors thank VECC Cyclotron staff for providing high quality beams during experiment and thankfully acknowledge the computing support received from the Lawrence Livermore National Laboratory (LLNL) Institutional Computing Grand Challenge program. J.S. acknowledges Niolas Schunck of LLNL for fruitful discussion. S.B. acknowledges with thanks the financial support received as Raja Ramanna Fellow from the Department of Atomic Energy, Government of India.

References

- [1] A. Bohr, B. Mottelson, Nuclear Structure, vol. II, Benjamin, Reading, MA, 1975.
- [2] R. Capote, et al., Nucl. Data Sheets 110 (2009) 3107.
- [3] A.J. Koning, S. Hilaire, S. Goriely, Nucl. Phys. A 810 (2008) 13.
- [4] A.V. Ignatyuk, K.K. Istekov, G.N. Smirenkin, Sov. J. Nucl. Phys. 29 (1979) 450.
- [5] G. Hansen, A.S. Jensen, Nucl. Phys. A 406 (1983) 236.
- [6] C. Ozen, Y. Alhassid, H. Nakada, Phys. Rev. Lett. 110 (2013) 042502.
- [7] S. Karampagia, V. Zelevinsky, Phys. Rev. C 94 (2016) 014321.
- [8] Alan L. Goodman, Phys. Rev. C 35 (1987) 2338(R).
- [9] Y. Alhassid, C.N. Gilbreth, G.F. Bertsch, Phys. Rev. Lett. 113 (2014) 262503.
- [10] S. Björnholm, A. Bohr, B. Mottelson, in: Proc. Int. Conf. on the Physics and Chemistry of Fission, vol. 1, Rochester, New York, 1973, IAEA, Vienna, 1974, p. 367.
- [11] A.R. Junghans, et al., Nucl. Phys. A 629 (1998) 635.
- [12] S. Komarov, et al., Phys. Rev. C 75 (2007) 064611.
- [13] Pratap Roy, et al., Phys. Rev. C 88 (2013) 031601(R).
- [14] J.L. Egido, L.M. Robledo, V. Martin, Phys. Rev. Lett. 85 (2000) 26.
- [15] J.C. Pei, W. Nazarewicz, J.A. Sheikh, A.K. Kerman, Phys. Rev. Lett. 102 (2009) 192501.
- [16] J.D. McDonnell, W. Nazarewicz, J.A. Sheikh, A. Staszczak, M. Warda, Phys. Rev. C 90 (2014) 021302(R).
- [17] N. Schunck, D. Duke, H. Carr, Phys. Rev. C 91 (2015) 034327.
- [18] Y. Alhassid, et al., Nucl. Phys. A 469 (1987) 205.
- [19] N. Dubrey, J. Dudek, A. Maj, Acta Phys. Pol. B 36 (2005) 1161.
- [20] Deepak Pandit, et al., Phys. Rev. C 81 (2010) 061302(R).
- [21] Soumik Bhattacharya, et al., Phys. Rev. C 95 (2017) 014301.
- [22] S. Das Gupta, et al., Phys. Rev. C 88 (2013) 044328.
- [23] P. Möller, J.R. Nix, W.D. Myers, W.J. Swiatecki, At. Data Nucl. Data Tables 59 (1995) 185.
- [24] K. Banerjee, T.K. Ghosh, S. Kundu, T.K. Rana, C. Bhattacharya, J.K. Meena, G. Mukherjee, P. Mali, D. Gupta, S. Mukhopadhyay, D. Pandit, S.R. Banerjee, S. Bhattacharya, T. Bandopadhyay, S. Chatterjee, Nucl. Instrum. Methods A 608 (2009) 440.
- [25] Deepak Pandit, et al., Nucl. Instrum. Methods A 624 (2010) 148.
- [26] K. Banerjee, et al., Phys. Rev. C 85 (2012) 064310.
- [27] Pratap Roy, et al., Phys. Rev. C 86 (2012) 044622.
- [28] Pratap Roy, K. Banerjee, C. Bhattacharya, R. Pandey, A. Sen, S. Manna, S. Kundu, T.K. Rana, T.K. Ghosh, G. Mukherjee, T. Roy, A. Dhal, A. Dey, J.K. Meena, A.K. Saha, Deepak Pandit, S. Mukhopadhyay, S. Bhattacharya, Phys. Rev. C 94 (2016) 064607.
- [29] R.J. Charity, Phys. Rev. C 82 (2010) 014610.
- [30] H.A. Bethe, Phys. Rev. 50 (1936) 332; H.A. Bethe, Rev. Mod. Phys. 9 (1937) 69.

- [31] A.V. Ignatyuk, G.N. Smirenkin, A.S. Tishin, Sov. J. Nucl. Phys. 21 (1975) 255.
- [32] Kurt A. Snover, Annu. Rev. Nucl. Part. Sci. 36 (1986) 545.
- [33] Deepak Pandit, et al., Phys. Lett. B 713 (2012) 434.
- [34] N. Schunck, J. Dobaczewski, W. Satula, P. Baczyk, J. Dudek, Y. Gao, M. Konieczka, K. Sato, Y. Shi, X.B. Wang, T.R. Werner, arXiv:1612.05314v2 [nucl-th], 19 Dec 2016.